TNF-α Inhibits Macrophage Clearance of Apoptotic Cells via Cytosolic Phospholipase A_2 and Oxidant-Dependent Mechanisms[1]

Kathleen McPhillips,* William J. Janssen,† Moumita Ghosh,‡ Aideen Byrne,‡ Shyra Gardai,‡ Linda Remigio,‡ Donna L. Bratton,‡ Jihee L. Kang,[2§] and Peter Henson[2,3‡]

Removal of apoptotic cells from inflammatory sites is an important step in the resolution of inflammation. Both murine and human macrophages stimulated with TNF-α or directly administered arachidonic acid showed an impaired ability to ingest apoptotic cells (efferocytosis). The inhibition was shown to be due to generation of reactive oxygen species, was blocked with a superoxide dismutase mimetic, MnTBAP, and was mimicked by direct addition of H_2O_2. To determine the mechanism of TNF-α-stimulated oxidant production, bone marrow-derived macrophages from gp91^{phox}-deficient mice were examined but shown to still produce oxidants and exhibit defective apoptotic cell uptake. In contrast, a specific cytosolic phospholipase A_2 inhibitor blocked the oxidant production and reversed the inhibited uptake. The suppressive effect of endogenous or exogenous oxidants on efferocytosis was mediated through activation of the GTPase, Rho. It was reversed in macrophages pretreated with C3 transferase to inactivate Rho or with an inhibitor of Rho kinase. During maturation of human monocyte-derived macrophages, only mature cells exhibited TNF-α-induced suppression of apoptotic cell clearance. The resistance of immature macrophages to such inhibition was shown to result not from defective generation of oxidants, but rather, from lack of response of these cells to the oxidants. Overall, the data suggest that macrophages in a TNF-α- and oxidant-rich inflammatory environment are less able to remove apoptotic cells and, thereby, may contribute to the local intensity of the inflammatory response. *The Journal of Immunology,* **2007, 178: 8117–8126.**

Programmed cell death, including apoptosis, is a mechanism for cell deletion to maintain normal tissue homeostasis as well as in pathophysiologic processes throughout the body. The apoptotic cells are removed by phagocytosis into both professional phagocytes (macrophages, other members of the mononuclear phagocyte system, and dendritic cells) or by so-called nonprofessional phagocytes (most tissue cells, including epithelial, endothelial, smooth muscle, stromal cells, and fibroblasts). Phagocytosis of apoptotic cells is an evolutionarily conserved process involving unique signaling pathways and uptake mechanisms that are different from ingestion involving Ig or C3 opsonization and Fc or C3 receptors (1–3). Among other differences, the uptake involves a spacious phagosome with concurrent ingestion of surrounding extracellular fluid and exhibits an obligatory participation of the low m.w. Rho family GTPase, Rac (4, 5). Of importance, ingestion of apoptotic cells is inhibited by activated RhoA (5–7). The process has been called efferocytosis (derived from effero, meaning to carry to the grave, to bury) (3, 8).

Inflammation involves influx of circulating inflammatory cells that must be removed during its resolution, a process that involves their apoptosis and local removal by macrophages and probably to some extent by endogenous tissue cells as well. TNF-α is a pleiotropic cytokine involved in stimulating inflammatory responses and is present at most inflammatory sites. It has been reported to enhance the uptake of apoptotic cells by immature monocyte-derived macrophages (9) and might therefore contribute to optimal clearance of apoptotic cells during resolution of inflammation. However, when we re-examined this phenomenon to address its mechanism, the effect of TNF-α on mature macrophages from mouse or human was to reduce the clearance of apoptotic cells rather than to enhance the uptake. The mechanisms underlying this biphasic response of immature vs mature macrophages to TNF-α represent the subject of this study. Because TNF-α is known to induce macrophage reactive oxygen species (ROS),[4] (10–12) and oxidants are present in acute inflammatory reactions, we sought a possible connection between the two and a possible role for oxidants in activation of Rho and suppression of efferocytosis.

Materials and Methods

Human subjects

The study was approved by, and performed in accordance with, the ethical standards of the institutional review board on human experimentation at the National Jewish Medical and Research Center (Denver, CO). Written informed consent was obtained from each subject.

*Department of Pathology, University of Colorado Health Sciences Center, Denver, CO 80262; †Division of Pulmonary Medicine, Department of Medicine, and ‡Program in Cell Biology, Department of Pediatrics, National Jewish Medical and Research Center, Denver, CO 80206; and §Department of Physiology, Ewha Womans University College of Medicine, Seoul, Korea

Received for publication December 6, 2006. Accepted for publication April 12, 2007.

The costs of publication of this article were defrayed in part by the payment of page charges. This article must therefore be hereby marked *advertisement* in accordance with 18 U.S.C. Section 1734 solely to indicate this fact.

[1] This work was supported by National Institutes of Health Grants GM61031, HL81151, AI058228, and HL34303.

[2] J.L.K. and P.H. are senior coauthors of this work.

[3] Address correspondence and reprint requests to Dr. Peter Henson, Department of Pediatrics, National Jewish Medical and Research Center, 1400 Jackson Street, Denver, CO 80206. E-mail address: hensonp@njc.org

[4] Abbreviations used in this paper: ROS, reactive oxygen species; HMDM, human monocyte-derived macrophage; BMDM, bone marrow-derived macrophage; DPI, diphenyleneiodonium; MnTBAP, manganese III tetrakis (5,10,15,20-benzoic acid) porphyrin; OTC, oxo-thiazolidine-carboxylic acid; DHE, dihydroethidium; C3T, C3 transferase; SOD, superoxide dismutase; $cPLA_2$, cytosolic phospholipase A_2; MAFP, methyl arachadonyl fluorophosphate.

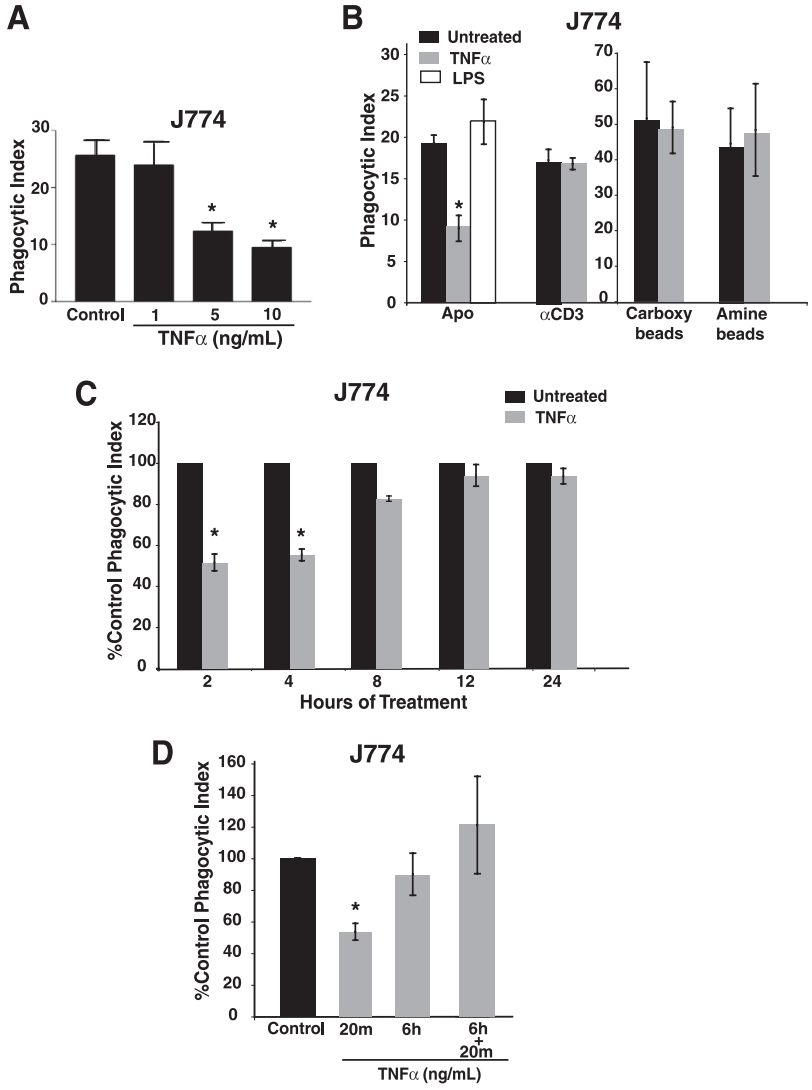

FIGURE 1. TNF-α inhibits engulfment of apoptotic cells specifically in a dose- and time-dependent manner. *A*, J774 macrophages were treated with TNF-α for 20 min, washed and apoptotic Jurkat cells added at a ratio of 10:1 for 90 min. *B*, J774 macrophages treated with 10 ng of LPS for 24 h showed no apoptotic cell engulfment defect. Apoptotic, opsonized, and bead targets were cocultured with J774 macrophages and only apoptotic cell engulfment was inhibited by TNF-α. *C*, J774 macrophages were left untreated or treated with TNF-α for various time points before analysis of uptake. *D*, After an initial TNF-α stimulation, J774s were treated again with TNF-α and the phagocytic index measured. TNF-α no longer inhibited engulfment after restimulation. Data represent the mean ± SEM ($n \geq 3$ experiments). *, $p < 0.05$.

Experimental animals

Mice were housed and studied under the Institutional Animal Care and Use Committee-approved protocols in the animal facility of National Jewish Medical and Research Center. Experiments were performed on 8- to 12-wk-old, age-matched mice.

Reagents

Recombinant mouse TNF-α (1–10 ng/ml) was obtained from R&D Systems. Human TNF-α (25 ng/ml) was purchased from BD Pharmingen. H_2O_2 (30%) from Sigma-Aldrich was used at 10 μM. Cells were viable based on trypan blue exclusion. LPS (*Escherichia coli* O111:B4) was from List Biological Laboratories and was used at 10 ng/ml for 24 h. Zymosan from Sigma-Aldrich was used at 25 particles per macrophage. In some assays, cells were pretreated with the following antioxidants: MnTBAP (manganese III tetrakis (5,10,15,20-benzoic acid) porphyrin); a superoxide dismutase (SOD) mimetic, at 50 μM (R&D Systems); diphenyleneiodonium (DPI), a flavoprotein inhibitor, at 5 μM (Sigma-Aldrich); and oxothiazolidine-carboxylic acid (OTC), an agonist of glutathione production, at 10 μM (Sigma-Aldrich). Dihydroethidium (DHE) was purchased from Molecular Probes and used to measure intracellular oxidant levels. C3T, an exoenzyme that ADP ribosylates RhoA, was purchased from Cytoskeleton. The Rho kinase inhibitor, LY27632, and pyrrolidine were purchased from Calbiochem and used at 10 μM for 30 min. Methyl arachadonyl fluorophosphate (MAFP) and arachidonic acid were purchased from Cayman Chemicals and used at 10 μM for 30 min or 100 μM for 20 min, respectively. PKH26 was purchased from Sigma-Aldrich and used at 10 μM.

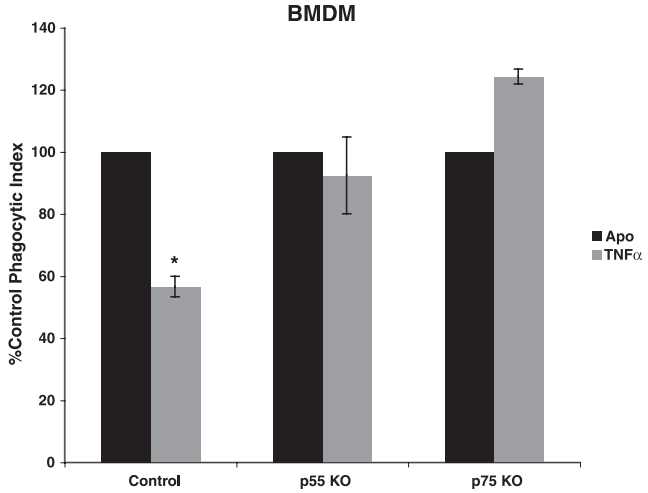

FIGURE 2. TNF-α can signal through both p55 and p75 to inhibit efferocytosis. BMDM from C57BL/6 control mice, $p55^{-/-}$ (TNFR1), and $p75^{-/-}$ (TNFR2) were treated with TNF-α for 20 min, washed, and apoptotic Jurkat T cells were added at a 10:1 ratio for 90 min. The phagocytic index was expressed as a percentage shown in untreated control. Data represent the mean ± SEM ($n \geq 3$ experiments). *, $p < 0.05$.

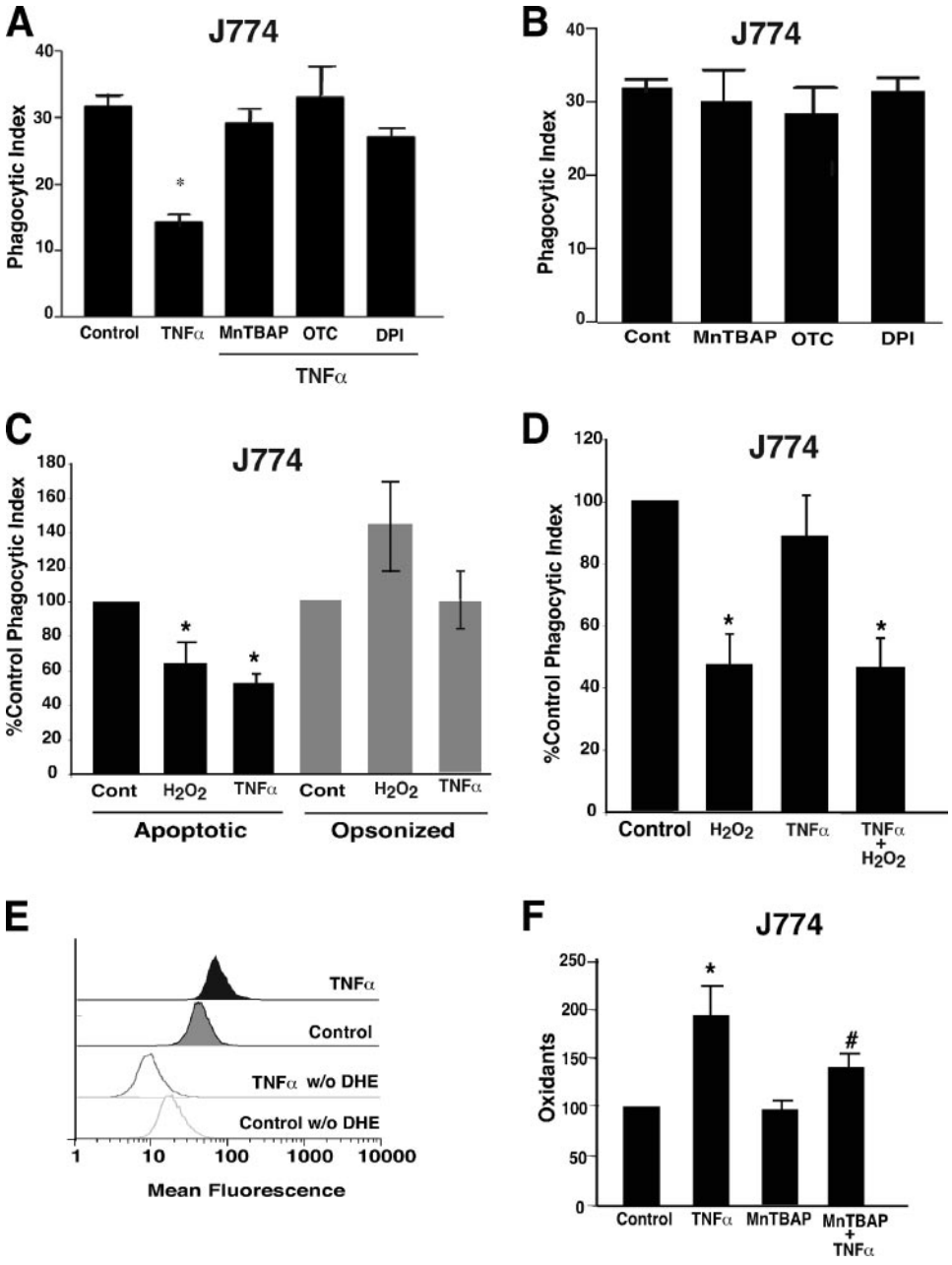

FIGURE 3. Antioxidants reverse both the level of oxidants and the engulfment defect in TNF-α-treated J774 macrophages. *A*, Three different antioxidants, MnTBAP (50 μM for 45 min), OTC (10 μM for 30 min), and DPI (10 μM for 30 min), reversed the engulfment defect observed in TNF-α-treated J774 macrophages. *B*, J774 cells treated with the antioxidants had no effect on efferocytosis alone. *C*, Exogenously added oxidants or TNF-α decreased clearance of apoptotic cells, but not IgG opsonized cells. *D*, After an initial TNF-α stimulation, J774 macrophages were treated with H_2O_2 and the phagocytic index measured. H_2O_2 inhibited engulfment after restimulation. *E*, J774 macrophages incubated with DHE for 3 h and analyzed by flow cytometry showed increased oxidant levels induced by 20 min of TNF-α stimulation. *F*, J774 macrophages analyzed with fluorescence microscopy showed increased oxidant levels induced by TNF-α stimulation. MnTBAP reversed the increase in oxidants. Quantification of DHE staining is expressed as a percentage of the control. Data represent the mean ± SEM ($n \geq 3$ experiments). *, $p < 0.05$ compared with control, #, $p < 0.05$ compared with TNF-α treated.

Cell culture

Murine J774 macrophages (American Type Culture Collection (ATCC)) were cultured in DMEM supplemented with 10% heat-inactivated FBS (ATCC), 2 mM L-glutamine, 100 μg/ml streptomycin, and 100 U/ml penicillin in humidified 10% CO_2 at 37°C. Human monocytes were isolated from whole blood using a Percoll gradient centrifugation, as previously described (13). Monocytes were plated in 24-well tissue culture plates (BD Biosciences), and matured to macrophages by culturing in X-Vivo medium (BioWhittaker) containing 10% human serum at 37°C in 10% CO_2 for 7 days. Medium was changed on days 3 and 6. All procedures to obtain human samples were Institutional Review Board approved. Human leukemia Jurkat T cell line was obtained from ATCC and was cultured in RPMI 1640 (Mediatech) containing 10% heat-inactivated FBS supplemented with 2 mM L-glutamine, 100 U/ml penicillin, and 100 μg/ml streptomycin (Sigma-Aldrich) in humidified 5% CO_2 at 37°C. Mouse bone marrow-derived macrophages (BMDM) were prepared and cultured in DMEM containing 10% (v/v) FBS and 10% (v/v) L cell-conditioned medium as a source of M-CSF for 5 days as previously described (14).

Induction of apoptosis and staining of thymocytes

Jurkat T cells were exposed to UV irradiation at 254 nm for 10 min and cultured for 2.5 h at 5% CO_2 at 37°C. Apoptosis was quantified by evaluation of nuclear morphology at the light microscopic level. By these methods, these cells were typically 70–90% apoptotic (7).

Murine thymocytes were isolated from the thymi of 8-wk-old, female C57BL/6 mice, by passing thymi through a 40-μm strainer to separate individual cells. Thymocytes were cultured in RPMI 1640 with 10% FCS at 3×10^6 cells/ml at 37°C in 5% CO_2 for 3 h after 10 min of UV irradiation. The thymocytes were washed with RPMI 1640 without serum and resuspended in Diluent C (Sigma-Aldrich) at 5×10^7 cells/ml and PKH26 linker solution was added to make a 10 μM solution. Cells were incubated at 37°C with gentle shaking for 15 min. RPMI 1640 with 10% FCS was added to stop the reaction and the cells were washed and resuspended in PBS with 0.1% BSA at 20×10^6 cells/ml.

Phagocytosis assay

Phagocytosis assays were performed as previously described (7). Approximately 0.5×10^5 J774 macrophages or 5×10^6 human monocyte-derived macrophage (HMDM) were plated in each well of a 24-well plate for 48 h or 7 days, respectively. The macrophages were washed with warm medium before treatment with TNF-α (10 ng/ml for 20 min), H_2O_2 (10 μM for 20 min), MnTBAP (50 μM for 30 min), DPI (5 μM for 30 min), OTC (10 μM for 30 min), or C3T (0.5 μg/ml for 48 h). The cells were washed three

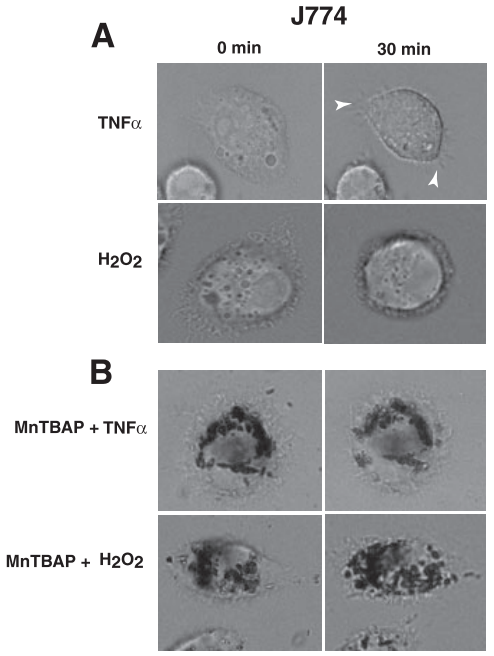

FIGURE 4. Oxidants induce morphologic changes within the J774 macrophages. The oxidant effects are reversed by the antioxidant, MnTBAP. *A*, Live microscopy showed cell shape changes in the TNF-α- and H_2O_2-treated J774 macrophages. The J774s rounded up, stopped ruffling, and started forming filopodia (arrowheads). *B*, J774 cells pretreated with MnTBAP (black pigment within the cells) maintained their shape and membrane ruffling after TNF-α and H_2O_2 treatment.

times before adding the following targets: apoptotic Jurkat T cells (resuspended in phagocyte medium) at a ratio of 10:1 (Jurkat T cells to phagocytes); anti-CD3 opsonized Jurkat T cells; 2 μl of 10-μm carboxylated beads (Polysciences), 2 μl of 10-μm aliphatic amine beads (Interfacial Dynamics). The phagocytes and either the cells or beads were cocultured for 90 min at 37°C in 5% CO_2, washed three times with PBS, and stained with a modified Wright's Giemsa stain (Fisher Scientific). The phagocytic index was calculated using the following formula: ((number of apoptotic bodies)/(200 total macrophages)) × 100 (15). Each condition was tested in duplicate and repeated at least three times.

Oxidant detection with DHE

DHE assays were performed according to a modified protocol from Sanlioglu et al. (16). Briefly, J774 cells (0.5×10^5 plated for 48 h) and HMDM at days 1 and 7 (5×10^6) were plated either on glass coverslips or directly on 30-mm glass-bottom dishes (MaTek) and incubated in whole medium containing 5 μM DHE and 5 μg/ml Hoescht (Sigma-Aldrich) for 3.5 h. Where indicated, TNF-α (10 ng/ml) or H_2O_2 (10 μM) were added for the last 20 min of incubation. For the last 30 min of incubation, MnTBAP (50 μM) was added. Cells were then washed three times with PBS and the coverslips were mounted in 1 ml of PBS in a glass-bottom dish and analyzed by confocal microscopy using a 40× objective. In the presence of intracellular oxidants, DHE is converted to ethidium and detected as bright red nuclear staining. The red DHE staining was quantified by creating masks and measuring fluorescent mean intensity of staining using Slidebook imaging software (Olympus). For the flow cytometry experiments, J774s were incubated in whole medium containing 5 μM DHE and 5 μg/ml Hoescht and treated with TNF-α (10 ng/ml) for 20 min. Cells were washed and scraped and oxidants were measured using the Cy3 channel and reported as the mean fluorescence.

Cytosolic phospholipase A_2 ($cPLA_2$) activation assays

Cells were plated at 0.5×10^5 in 24-well culture plates and analyzed for [^{3}H]arachidonic acid release as previously described (17). Cells were labeled in serum-free medium supplemented with 0.5 μCi/ml [^{3}H]arachidonic acid. Cells were left to incorporate the [^{3}H]arachidonic acid into their membrane lipids overnight followed by three washes with DMEM and 1% BSA. Cells were then incubated with 10 ng/ml TNF-α for the indicated times. After treatment, the medium was removed from the plates and centrifuged at $1600 \times g$ for 3 min at 4°C to pellet any detached cells. The supernatants were assessed for [^{3}H]arachidonic acid and product release by liquid-scintillation counting.

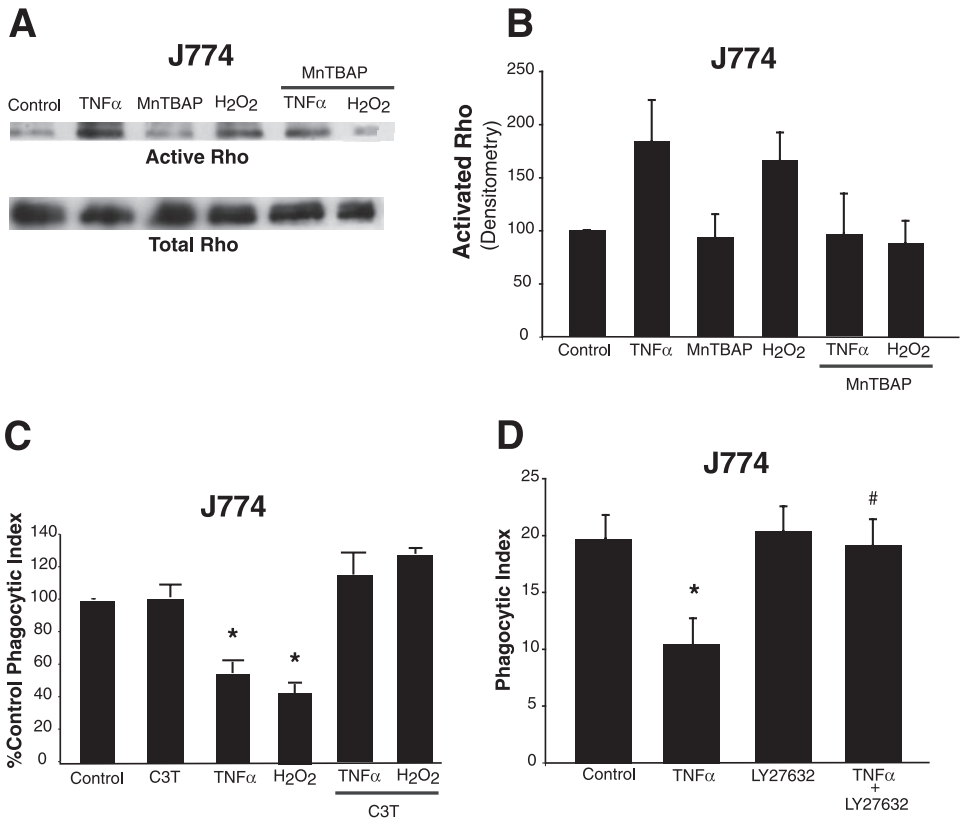

FIGURE 5. TNF-α-induced oxidants activate Rho. *A* and *B*, J774 macrophages were untreated or treated with TNF-α, H_2O_2, or with or without MnTBAP. MnTBAP reversed the TNF-α- and H_2O_2-induced Rho activation. Representative blots are shown from four separate experiments. Densitometry numbers were calculated by measuring the ratio of active protein to total protein and expressed as a proportion of the number in untreated control. *C*, The specific Rho inhibitor C3T reversed the clearance defect observed in TNF-α or H_2O_2 treated J774 macrophages. *D*, J774 cells treated with 10 μM LY27632 (Rho kinase inhibitor) reversed the TNF-α-induced inhibition. Data represent the mean ± SEM ($n \geq 3$ experiments). *, $p < 0.05$ compared with control; #, $p < 0.05$ compared with TNF-α-treated.

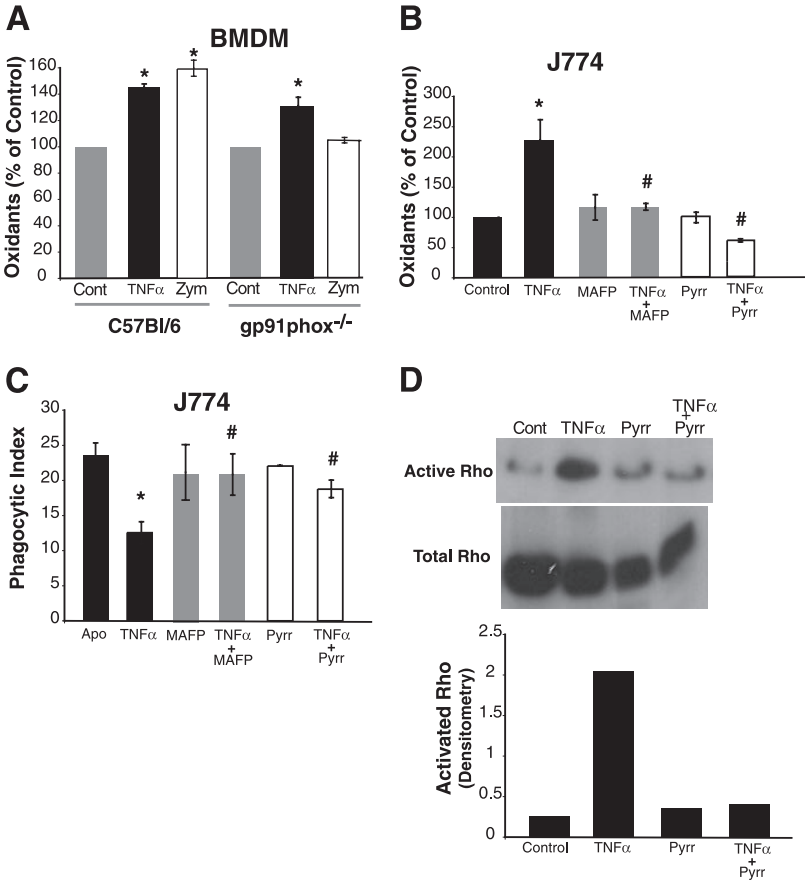

FIGURE 6. The TNF-α-induced oxidants were generated through the $cPLA_2$ pathway. *A*, BMDM from C57BL/6 and $gp91^{phox}$-deficient mice treated with TNF-α or zymosan (25 particles/cell) for 20 min were measured for oxidant levels. TNF-α induced oxidant production in both cell types while zymosan induced oxidants in the control mice, but not in the $gp91^{phox}$-deficient mice. *B*, J774 macrophages treated with a general phospholipase inhibitor, MAFP, or a specific $cPLA_2$ inhibitor, pyrrolidine (Pyrr, 1 μM for 30 min), showed reversal of the TNF-α-induced oxidant generation. *C*, J774 macrophages pretreated with MAFP or pyrrolidine before TNF-α reversed the efferocytosis defect. Data represent the mean $\pm$ SEM ($n \geq 3$ experiments). $*$, $p < 0.05$ compared with control, #, $p < 0.05$ compared with TNF-α treated. *D*, Western blot analysis of active Rho from J774 lysates treated with TNF-α (10 ng/ml for 20 min) or pyrrolidine (1 μM for 30 min). Densitometry numbers were calculated by measuring the ratio of active protein to total protein and expressed as a percentage of oxidant in the untreated control (Cont). Blots shown were representative of four experiments.

Rho and Rac activity assays

Rho and Rac activity assays were performed according to the manufacturer's indications (Millipore). Briefly, 2.5×10^6 J774 macrophages were plated for 2 days and where indicated stimulated with TNF-α (10 ng/ml) and H_2O_2 (10 μM) for 20 min or MnTBAP (50 μM) for 30 min. Samples were lysed and active Rho was isolated using Sepharose-bound Rhotekin and active Rac was isolated using Sepharose-bound p21-activated protein kinase. Lysates were incubated for 1 h, washed, boiled, and run on a 12% SDS-PAGE gel. To ensure equal loading, 50 μl of whole cell lysate were run on the gel for each condition and total Rho and total Rac levels were evaluated.

Videomicroscopy

J774 macrophages or HMDM were cultured on Delta T dishes (Bioptechs) for 2 days (J774) or 1–7 days (HMDM). The cells were placed on a 37°C heated stage and analyzed using a 60× oil objective on an Olympus IX70 inverted microscope. After 10 min, TNF-α (10 ng/ml) or H_2O_2 (10 μM) were injected into the dish and the cells were analyzed for an additional 20 min. Pictures were recorded every 15 s for a total of 30 min using TILLvisION software. For the MnTBAP videos, the macrophages were pretreated with MnTBAP (50 μM) for 20 min at 37°C in a 5% CO_2 incubator before being placed on the 37°C heated stage. The MnTBAP samples were analyzed for 10 min on the heated stage before TNF-α or H_2O_2 were injected into the dish. All images were saved as tiff files.

Densitometry analysis

Western blots were scanned and analyzed using ImageJ analysis from the National Institutes of Health. The scans were inverted and the background was subtracted before measuring the relative protein amounts. Densitometry numbers were calculated by measuring the ratio of active protein to total protein. All conditions were expressed as a percentage of the untreated control.

In vivo experiments

C57BL/6 mice were i.p. injected with 50 ng of TNF-α in 500 μl of PBS with 0.1% BSA (Sigma-Aldrich) or 500 μl of PBS with 0.1% BSA for 30 min. The mice were then injected with 10×10^6 apoptotic thymocytes (i.p.) in 500 μl of PBS with 0.1% BSA. After 1 h, the mice were sacrificed and the peritoneal cells were lavaged using 5 ml of PBS with 0.1% BSA. The peritoneal lavages were cytospun and stained. Phagocytosis was measured by counting the number of apoptotic bodies within at least 200 macrophages using light microscopy.

Statistical analysis

All experiments were performed at least three times. Statistical analysis and *p*-value calculations were conducted using the JMP statistical program (SAS Institute). The Dunnett's and Tukey-Kramer parametrical tests were used for single and multiple comparisons, respectively. Experiments with a value $p < 0.05$ indicated by asterisk are the experimental sample compared with control. Experiments using a number sign to indicate a value $p < 0.05$ represent the experimental sample compared with the TNF-α sample.

Results

TNF-α inhibits efferocytosis in a dose- and time-dependent manner

A murine macrophage cell line, J774, was used to examine the effects of TNF-α on uptake of apoptotic cells. After pretreatment with TNF-α followed by washing, the J774 cells were cocultured with apoptotic cells for 90 min. TNF-α inhibited uptake of apoptotic cells in a dose-dependent manner (Fig. 1*A*) and 10 ng/ml was used for the remaining experiments. To determine whether the TNF-α inhibitory effects were specific to apoptotic cells, several other target cells were analyzed. Anti-CD3 opsonized viable Jurkat T cells, carboxylated beads, and amine beads were taken up readily in both the untreated and TNF-α treated groups. LPS was also added to the macrophages to show that the inhibitory effects were specific to TNF-α and not a general macrophage activator (Fig. 1*B*). To examine the duration of TNF-α inhibition, the phagocytic

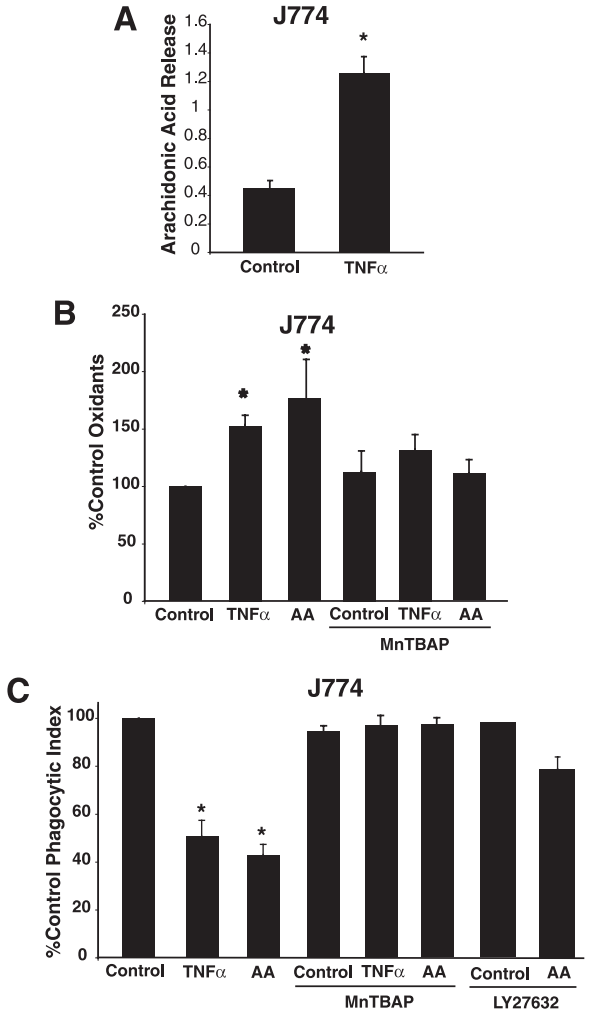

FIGURE 7. Release of arachidonate products and reversal of arachidonate-induced oxidant generation and decreased efferocytosis by an antioxidant. *A*, Arachidonic acid release was measured in TNF-α stimulated J774 macrophages. *B*, Arachidonic acid (AA, 100 μM) added to macrophages for 20 min increased oxidant levels in J774 macrophages. These were decreased with MnTBAP pretreatment. *C*, Direct addition of arachidonic acid to J774 macrophages inhibited engulfment of apoptotic cells. This defect was reversed using the antioxidant, MnTBAP or the Rho kinase inhibitor, LY27632. Data represent the mean ± SEM, $n \geq 3$. *, $p < 0.05$ compared with control.

index of J774 cells was analyzed over the course of 24 h. Efferocytosis was inhibited up to 4 h after pretreatment with TNF-α. By 8 h of incubation, the inhibitory effects were no longer observed (Fig. 1*C*). During the recovery period, the J774 cells were restimulated with TNF-α for 20 min without further inhibitory effect, showing that the recovery was not due to loss of TNF-α from the system (Fig. 1*D*). The macrophages did not have an eating defect after TNF-α restimulation.

TNF-α signaling through both p55- and p75-inhibited efferocytosis

The homotrimeric TNF-α ligand signals through two distinct cell surface receptors: TNFR1 (p55) and TNFR2 (p75). p55 is mainly thought to be associated with soluble TNF-α, whereas p75 is associated with membrane-bound TNF-α (18). To determine which receptor was signaling to inhibit engulfment of apoptotic cells, murine BMDMs were harvested from $p55^{-/-}$, $p75^{-/-}$, and C57BL/6 controls. After 5 days in culture the mature macrophages were treated with TNF-α and cocultured with apoptotic Jurkat T cells. TNF-α reduced engulfment of apoptotic cells in the control macrophages, but not in either the $p55^{-/-}$ or $p75^{-/-}$ cells, suggesting that exogenously added soluble TNF-α requires both TNFRs to optimally inhibit apoptotic cell engulfment (Fig. 2).

Antioxidants reversed both the TNF-α-induced ROS generation and the efferocytosis inhibition in J774 macrophages

Several reports have shown that TNF-α alters the redox state of cells (19–21) and the resulting ROS can act as signaling molecules. J774 cells pretreated with a variety of antioxidants before TNF-α stimulation were no longer blocked in their ability to engulf apoptotic cells (Fig. 3*A*). The antioxidants alone had no effect on efferocytosis (Fig. 3*B*). To verify that engulfment was inhibited by ROS, exogenous H_2O_2 was directly added to J774 macrophages before the addition of apoptotic Jurkat T cells. This resulted in significant inhibition of the uptake of apoptotic cells (Fig. 3*C*). This concentration and duration of H_2O_2 treatment did not affect the viability of the J774 cells as indicated by trypan blue exclusion. The TNF-α- or H_2O_2-treated J774 cells were still able to engulf IgG opsonized cells (Fig. 3*C*), suggesting the oxidant-mediated engulfment defect is specific for apoptotic cells. Because both TNF-α and oxidants are present during an inflammatory response, the effects of both stimuli were analyzed. J774s were first stimulated with TNF-α and after 6 h were restimulated with H_2O_2. Unlike the TNF-α restimulation results in Fig. 1*C*, H_2O_2 restimulation was still able to inhibit uptake, showing that exogenous sources of ROS continue to exert effects on macrophages after the TNF-α effects have waned (Fig. 3*D*). To confirm that TNF-α inhibition was due to intracellular ROS generation, J774 cells were treated with DHE and Hoescht stains. DHE passes freely into live cells and rapidly reacts with intracellular oxidants resulting in the generation of ethidium, which intercalates into the DNA and fluoresces in the Cy3 (red) channel. The cells were either left untreated or treated with TNF-α and analyzed using either flow cytometry or fluorescent microscopy. We found a significant increase in the level of oxidant staining in the TNF-α treated J774s compared with the untreated control cells (Fig. 3*E*). This finding was reversed with MnTBAP pretreatment (Fig. 3*F*). Using Slidebook software the amount of oxidant staining was quantified within the cells. TNF-α increased the staining by 100%, whereas MnTBAP substantially decreased the oxidant levels (Fig. 3*F*). These data suggest that TNF-α stimulation induces oxidant production leading to an inhibition of uptake of apoptotic cells.

TNF-α and H_2O_2 induced morphologic changes in J774 macrophages that were reversed with MnTBAP

Various external stimuli have been shown to alter the morphologic phenotype of macrophages which in turn governs the functions of the cells (22, 23). Accordingly, J774 macrophages were examined by videomicroscopy after TNF-α or oxidant addition. After monitoring the macrophages for 10 min, TNF-α or oxidants were added for 20 min and morphological cell changes were analyzed. The untreated J774 cells were slightly extended and ruffled around the edges. With the addition of TNF-α the cells rounded up, stopped ruffling and began to form filopodia (Fig. 4*A*). Morphological differences were also observed with the addition of H_2O_2. Because the antioxidant MnTBAP was shown to reverse the engulfment defect induced by TNF-α, J774 macrophages were pretreated with MnTBAP before the addition of TNF-α or H_2O_2. Pretreatment with MnTBAP reversed the cell shape changes (Fig. 4*B*) induced by TNF-α or H_2O_2. The cells maintained their extended and ruffling phenotype even after TNF-α or H_2O_2 addition.

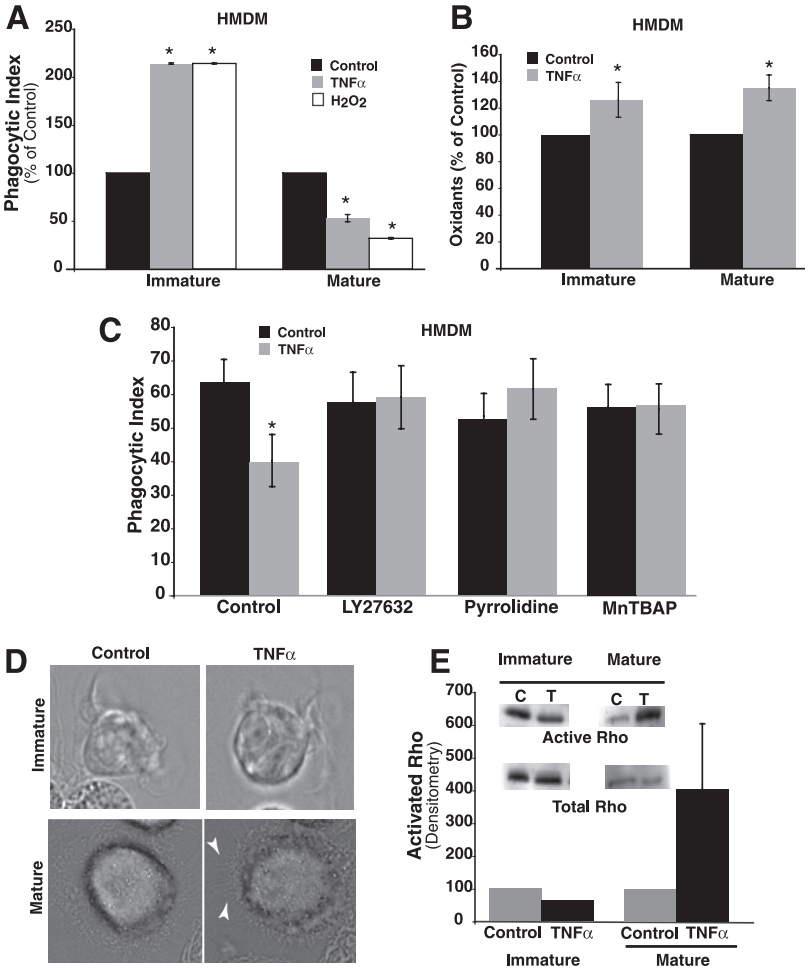

FIGURE 8. Mature HMDMs (day 7) have defective clearance of apoptotic cells, whereas immature HMDMs (day 1) have enhanced clearance of apoptotic cells in response to TNF-α and H_2O_2. *A*, Immature monocytes or mature macrophages were pretreated with TNF-α or H_2O_2 for 20 min before apoptotic Jurkat cells were added. Monocytes showed enhanced engulfment, whereas mature macrophages showed decreased engulfment. *B*, Both mature HMDMs and immature monocytes have significantly enhanced oxidant levels with TNF-α stimulation. Data represent the mean $\pm$ SEM ($n \geq 3$ experiments). $*$, $p < 0.05$ compared with control. *C*, Mature macrophages pretreated with Rho kinase inhibitor (LY27632), $cPLA_2$ inhibitor (pyrrolidine), or the antioxidant (MnTBAP) before addition of TNF-α showed a reversal in the TNF-α-induced engulfment defect. *D*, Live microscopy showed cell shape changes in TNF-α-treated HMDMs. Mature HMDMs stopped ruffling, and started forming filopodia (arrowheads). Immature HMDMs continued ruffling after TNF-α treatment. *E*, Rho activity was measured for mature and immature HMDMs either untreated or treated with human TNF-α. There were no significant changes in Rho activity in the immature macrophages, but there was an increase in the amount of active Rho in the TNF-α treated mature macrophages. C, Control; T, TNF-α-treated. Representative blots are shown from four separate experiments. Densitometry numbers were calculated by measuring the ratio of active protein to total protein and expressed as a percentage of the untreated control.

Oxidants induced Rho activation leading to an inhibition of efferocytosis, which was reversed using a Rho inhibitor or an antioxidant

The family of small Rho GTPases has been implicated in cellular shape changes in various cell types including macrophages. The morphologic changes observed after TNF-α or H_2O_2 addition correlate to changes in cellular Rho GTPases. Rac1 is required for membrane ruffling and efferocytosis, whereas Rho activation leads to filopodia formation and decreased efferocytosis (4–6). To determine whether the observed phenotype changes were Rho-mediated, active GTP-bound Rho was measured. J774 macrophages were either unstimulated or stimulated with TNF-α, H_2O_2, MnTBAP, or a combination of TNF-α and MnTBAP or H_2O_2 and MnTBAP. Both TNF-α and H_2O_2 increased the amount of active Rho in the J774 macrophages compared with control (Fig. 5*A*). This increase was reversed with the addition of the antioxidant, MnTBAP. TNF-α and H_2O_2 increased RhoA activity by 75 and 65%, respectively (Fig. 5*B*). These data suggest that TNF-α induces oxidant production, which in turn activates Rho. Rho effects have been analyzed previously using the Rho kinase inhibitor (LY27632) and the direct inhibitor of RhoA, C3 transferase (6). To determine the effects of Rho activation on efferocytosis in this system, J774 cells were treated with both LY27632 and C3 transferase. Preincubation of these cells for 48 h with C3T lead to Rho inactivation even without the inclusion of a protein transporter (data not shown). As expected, both the TNF-α and H_2O_2 inhibited engulfment of apoptotic cells. However, pretreatment with C3T reversed this inhibition and restored the ability of the macrophages to engulf apoptotic cells (Fig. 5*C*). To analyze the effects on engulfment by a downstream target of Rho, an inhibitor of Rho kinase (LY27632) was added to the system. This inhibitor also reversed the efferocytosis defect observed after TNF-α stimulation (Fig. 5*D*).

TNF-α-induced oxidants were generated through the $cPLA_2$ pathway

Several reports have linked TNF-α signaling to ROS generation through either the NADPH oxidase complex or mitochondria (10–12). To investigate the role of NADPH oxidase in TNF-α-induced ROS generation, $gp91^{phox-/-}$ BMDM were treated with TNF-α. Interestingly, the BMDM were still able to generate oxidants in response to TNF-α, but not to zymosan in the absence of gp91, a critical component of the NADPH oxidase (Fig. 6*A*). Western blots confirmed the absence of $gp91^{phox}$ in the macrophages. These data suggested an alternative mechanism of ROS production after TNF-α stimulation. To test other sources of oxidants, J774 cells were treated with antimycin A or rotenone (mitochondrial electron transport inhibitors) and again, oxidants were still generated in response to TNF-α (data not shown). A number of investigators have suggested that the phospholipase $cPLA_2$ is activated after TNF-α stimulation and can contribute to ROS production through the liberation and subsequent metabolism of arachidonic acid (24, 25). The role of $cPLA_2$ in the generation of ROS was tested in J774 macrophages. The cells had decreased TNF-α-induced oxidant generation after treatment with MAFP, a general phospholipase inhibitor, or pyrrolidine, a specific inhibitor of $cPLA_2$ (Fig. 6*B*).

TNF-α-induced oxidant generation was also diminished in the wild-type and gp91$^{phox-/-}$ BMDM treated with pyrrolidine (data not shown). These data demonstrated that TNF-α signaling through cPLA$_2$ led to increased levels of ROS. Decreasing the cPLA$_2$ activity using MAFP or pyrrolidine also reversed the TNF-α induced engulfment defect (Fig. 6*C*). To analyze the downstream signaling of cPLA$_2$ activation, Rho was measured using lysates from J774s treated with TNF-α or the cPLA$_2$ inhibitor, pyrrolidine. The increase in Rho activity observed after TNF-α treatment was reduced to control levels with pyrrolidine pretreatment (Fig. 6*D*) suggesting a role for ROS generated through the cPLA$_2$ pathway in signaling and activation of Rho.

Arachidonic acid released by cPLA$_2$ induces oxidant production and inhibits efferocytosis

To verify that TNF-α was activating the cPLA$_2$ pathway, the products of cPLA$_2$ activation, free arachidonic acid and arachidonate products, were measured. J774s were treated with [^{3}H]arachidonic acid overnight before TNF-α stimulation. The supernatants were analyzed for labeled liberated arachidonate products. TNF-α increased arachidonic acid release by 3.5-fold over the untreated control cells (Fig. 7*A*). Similar to TNF-α stimulation, arachidonic acid added to the J774 macrophages generated oxidants and decreased efferocytosis in a dose-dependent manner (data not shown). The oxidant effects were reversed with the antioxidant MnTBAP (Fig. 7*B*), and the TNF-α inhibitory effects were reversed with both MnTBAP and the Rho kinase inhibitor LY27632 (Fig. 7*C*), again demonstrating the role of ROS and Rho in inhibiting macrophage engulfment of apoptotic cells. Preliminary data suggests that both the lipoxygenase and cyclooxygenase enzyme families use arachidonic acid as a substrate during the generation of oxidants, but the exact mechanism is beyond the scope of this study.

Monocytes and mature macrophages respond differently to TNF-α and H_2O_2 treatment

To determine whether TNF-α inhibited efferocytosis in a human model, monocytes were isolated from whole blood and matured into macrophages over a period of 7 days. The mature macrophages showed decreased engulfment of apoptotic cells after either TNF-α or H_2O_2 treatment (Fig. 8*A*). Interestingly, Ren and Savill (9) have shown an increase in engulfment of apoptotic cells in immature monocytes treated with TNF-α. These results were verified in this study as shown in Fig. 8*A*. The differences in engulfment between immature and mature macrophages were explored by analyzing ROS generation and Rho activation. TNF-α stimulation resulted in increased ROS production in both immature and mature human macrophages (Fig. 8*B*). Mature HMDM pretreated with the Rho kinase inhibitor (LY27632), the cPLA$_2$ inhibitor (pyrrolidine), or the antioxidant (MnTBAP) were able to reverse the TNF-α induced defect in efferocytosis as observed previously in the murine BMDM. Although both immature and mature macrophages enhanced oxidants levels in response to TNF-α, the Rho activation differed between the two cell types. The mature human macrophages had enhanced Rho activity after TNF-α stimulation (Fig. 8*E*), whereas active Rho levels in immature monocytes remained unchanged after TNF-α stimulation (Fig. 8*E*). Videomicroscopy further demonstrated the differences between the two cell types. Immature monocytes continued ruffling after TNF-α treatment and looked the same as the untreated control (Fig. 8*D*). The mature macrophages, however, ruffled in the untreated control, but began to shrink and produce filopodia upon TNF-α treatment (Fig. 8*D*).

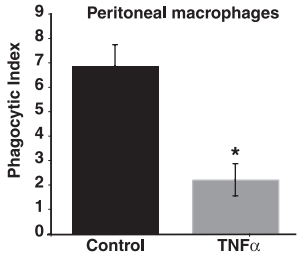

FIGURE 9. TNF-α inhibits engulfment of apoptotic cells in vivo. C57BL/6 mice ($n = 9$) were i.p. injected with 50 ng of TNF-α in 500 μl of PBS/0.1% BSA or 500 μl of PBS/0.1% BSA. After 30 min, 10×10^6 apoptotic thymocytes were i.p. injected. After 1 h of incubation, the mice were sacrificed and the peritoneal cells were lavaged. The peritoneal lavages were cytospun and stained and phagocytosis was measured using light microscopy. Data represent the mean ± SEM. *, $p < 0.05$ compared with control.

To further verify the TNF-α inhibitory studies, the effects of TNF-α on efferocytosis in vivo were analyzed. C57BL/6 mice were i.p. injected with either TNF-α or the PBS control for 30 min. PKH26 labeled apoptotic thymocytes were then i.p. injected for 1 h before the peritoneum was lavaged. The cells were spun down and the phagocytic index was calculated as described in *Materials and Methods*. There was a 3-fold decrease in efferocytosis in the TNF-α-treated mice (Fig. 9). The inhibitory effects of TNF-α on macrophage function were observed both in vitro and in vivo.

Discussion

This work describes a mechanism by which TNF-α and oxidants inhibit the clearance of apoptotic cells by macrophages. The model (Fig. 10) shows the dependence on cPLA$_2$ for oxidant generation and an involvement of Rho in the suppression of uptake. Intriguingly, only mature macrophages were responsive to this TNF-α

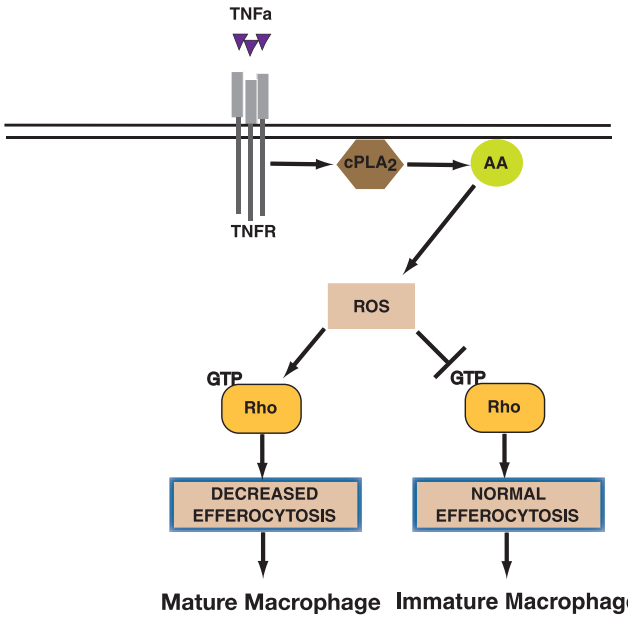

FIGURE 10. Illustrative representation of the TNF-α signaling pathway leading to the suppression of efferocytosis. The homotrimer, TNF-α, activates the TNFR which in turn activates the enzyme cPLA$_2$ leading to the cleavage and release of arachidonic acid. During this process, oxidants that induce conversion of Rho from the inactive GDP state to the active GTP state are produced. The active Rho causes morphologic changes within the cell preventing the mature macrophage from engulfing apoptotic cells.

and oxidant effect. We speculate that TNF-α and exogenous oxidants present in inflammatory lesions can block the local clearance of apoptotic cells by mature macrophages at the site but would have little effect on incoming and maturing monocytes. Importantly, the effect of TNF-α and oxidants was specific for apoptotic cell uptake (efferocytosis) and did not apply to phagocytosis of IgG opsonized cells, carboxylated beads, or aliphatic amine beads through FcRs.

An important outcome from these experiments is the demonstration that endogenous and exogenous oxidants can inhibit uptake of apoptotic cells. Thus there are many situations of altered redox state in tissues that may generate similar suppression of apoptotic cell clearance, with clear implications for persistence of inflammation and/or release of intracellular contents from apoptotic cells that are not removed and, therefore, undergo secondary necrosis. Furthermore, although TNF-α seemed to be inducing endogenous oxidants via effects on $cPLA_2$ and release of arachidonate, one may reasonably presume that stimuli that induce oxidants through NADPH oxidase or mitochondrial pathways would have similar suppressive effects. Indeed, stimulation of macrophages with zymosan (a potent NADH oxidase activator) also was found to block apoptotic cell uptake (Fig. 6*A*) although the system is complicated by the concurrent ingestion of the zymosan particles used to stimulate the oxidant response.

The oxidants, generated from TNF-α stimulation or direct administration of H_2O_2 led to activation of Rho. This effect of altered redox state on Rho has been observed previously (26–28), although the mechanisms of signal transmission to the GTPase are not known. A novel (GXXXXXGK(S/T)C motif was discovered in nearly 50% of all Rho subfamily GTPases that contains a cysteine residue that may be the direct target of ROS (28). There are several conflicting reports in the literature about the relationship of ROS and RhoGTPases. Nimnual et al. (26) demonstrated a down-regulation of Rho by Rac-induced ROS in HeLa cells. However, another study reported an increase in Rho activation by ROS in rat aortic rings (27). A recent article reported that H_2O_2 is able to regulate both phosphatase and protein kinase activities (29), which could readily affect downstream RhoGTPase signaling. There are a large number of potential RhoGEFs and RhoGAPs that could be the ultimate mediators of this effect. We and others have shown that activated Rho can block efferocytosis and that Rac and Rho act in a balance to enhance (mediate) or inhibit uptake of apoptotic cells. Thus, in the experiments reported in this study, direct inhibition of Rho or of Rho kinase, resulted in a reversal of the inhibition. The small GTPases of the Rho family are key regulators of not only phagocytosis, but also of cytoskeletal changes, cell adhesion, gene expression, cell cycle, and cell survival (30, 31). Activation of RhoA is typically followed by stress fiber formation in many cell types (32), which appear to render a cell incapable of apoptotic cell engulfment.

Importantly, the immature macrophages were not defective in generation of oxidants but, rather, appeared to be unresponsive to them as far as Rho activation was concerned. In the future, this defect may provide clues to the pathways from oxidants to Rho. It should be noted that although the effect of TNF-α on blocking apoptotic cell uptake was transient, and the cells were then refractory to further additions of the cytokine, repeated additions of H_2O_2 were still able to inhibit uptake. Thus, a later inability of oxidants to activate Rho (as seen in the immature macrophages) was not the explanation for the transient nature of the TNF-α effect or the later refractoriness to this stimulus. Rather, we suspect down-regulation or desensitization of the TNF-α receptors to explain this phenomenon. Teleologically, this may be important in an inflammatory lesion where a transient blockade of macrophage efferocytosis would prevent the cells from becoming preoccupied in removing apoptotic cells, therefore, freeing them to ingest foreign organisms and opsonized material until the resolution stage in which removal of the apoptotic inflammatory cells becomes critical.

The generation of oxidants by TNF-α appeared to proceed, not from activation of NADPH oxidase or mitochondrial pathways, but rather as a result of $cPLA_2$ effects. This enzyme results in release of arachidonic acid and in these studies, direct addition of the fatty acid had the same effect in stimulating oxidant generation as well as blockade of efferocytosis. A number of oxidases and peroxidases act on arachidonate and in so doing, generate oxidants (33, 34). These include the cyclooxygenase and lipoxygenase enzyme families (35). Because there is significant redundancy among these enzymes in macrophages we did not attempt to address which specific ones were involved, although 12/15 lipoxygenase is likely to be a major participant. Examination of cells from TNF-α receptor-deficient mice suggested that both TNFRI and TNFRII were involved together in the optimal suppressive effect. In most circumstances, TNFRI appears to the predominant activating receptor for TNF-α, but a number of situations have been reported in which TNFRII can participate as a potential partner in cell stimulation (36, 37). Both TNFRI and TNFRII have been shown to be involved in $cPLA_2$ activation. A novel death domain protein, MADD, was shown to interact with TNFRI leading to activation of ERK and c-Jun causing the phosphorylation of $cPLA_2$ (38). TNFRII, however, was shown to activate $cPLA_2$ by translocating it to the plasma membrane leading to a calcium efflux rather than through a MAPK-dependent mechanism (24).

The data presented provide a novel mechanism by which TNF-α inhibits the engulfment of apoptotic cells both in vitro and in vivo. TNF-α stimulation of mature macrophages induces oxidant production through $cPLA_2$ activation and arachidonic acid release leading to increased active Rho and decreased efferocytic function.

Disclosures

The authors have no financial conflict of interest.

References

1. Savill, J., I. Dransfield, C. Gregory, and C. Haslett. 2002. A blast from the past: clearance of apoptotic cells regulates immune responses. *Nat. Rev. Immunol.* 2: 965–975.
2. Henson, P. M. 2005. Engulfment: ingestion and migration with Rac, Rho and TRIO. *Curr. Biol.* 15: R29–R30.
3. deCathelineau, A. M., and P. M. Henson. 2003. The final step in programmed cell death: phagocytes carry apoptotic cells to the grave. *Essays Biochem.* 39: 105–117.
4. Abell, A. N., A. M. deCathelineau, S. A. Weed, D. R. Ambruso, D. W. Riches, and G. L. Johnson. 2004. Rac2D57N, a dominant inhibitory Rac2 mutant that inhibits p38 kinase signaling and prevents surface ruffling in bone-marrow-derived macrophages. *J. Cell Sci.* 117: 243–255.
5. Nakaya, M., M. Tanaka, Y. Okabe, R. Hanayama, and S. Nagata. 2006. Opposite effects of rho family GTPases on engulfment of apoptotic cells by macrophages. *J. Biol. Chem.* 281: 8836–8842.
6. Tosello-Trampont, A. C., K. Nakada-Tsukui, and K. S. Ravichandran. 2003. Engulfment of apoptotic cells is negatively regulated by Rho-mediated signaling. *J. Biol. Chem.* 278: 49911–49919.
7. Hoffmann, P. R., A. M. deCathelineau, C. A. Ogden, Y. Leverrier, D. L. Bratton, D. L. Daleke, A. J. Ridley, V. A. Fadok, and P. M. Henson. 2001. Phosphatidylserine (PS) induces PS receptor-mediated macropinocytosis and promotes clearance of apoptotic cells. *J. Cell Biol.* 155: 649–659.
8. Gardai, S. J., K. A. McPhillips, S. C. Frasch, W. J. Janssen, A. Starefeldt, J. E. Murphy-Ullrich, D. L. Bratton, P. A. Oldenborg, M. Michalak, and P. M. Henson. 2005. Cell-surface calreticulin initiates clearance of viable or apoptotic cells through trans-activation of LRP on the phagocyte. *Cell* 123: 321–334.
9. Ren, Y., and J. Savill. 1995. Proinflammatory cytokines potentiate thrombospondin-mediated phagocytosis of neutrophils undergoing apoptosis. *J. Immunol.* 154: 2366–2374.
10. Finkel, T. 2003. Oxidant signals and oxidative stress. *Curr. Opin. Cell Biol.* 15: 247–254.
11. Garg, A. K., and B. B. Aggarwal. 2002. Reactive oxygen intermediates in TNF signaling. *Mol. Immunol.* 39: 509–517.

12. Goossens, V., J. Grooten, K. De Vos, and W. Fiers. 1995. Direct evidence for tumor necrosis factor-induced mitochondrial reactive oxygen intermediates and their involvement in cytotoxicity. *Proc. Natl. Acad. Sci. USA* 92: 8115–8119.
13. Haslett, C., L. A. Guthrie, M. M. Kopaniak, R. B. Johnston, Jr., and P. M. Henson. 1985. Modulation of multiple neutrophil functions by preparative methods or trace concentrations of bacterial lipopolysaccharide. *Am. J. Pathol.* 119: 101–110.
14. Riches, D. W., and G. A. Underwood. 1991. Expression of interferon-β during the triggering phase of macrophage cytocidal activation: evidence for an autocrine/paracrine role in the regulation of this state. *J. Biol. Chem.* 266: 24785–24792.
15. Fadok, V. A., J. S. Savill, C. Haslett, D. L. Bratton, D. E. Doherty, P. A. Campbell, and P. M. Henson. 1992. Different populations of macrophages use either the vitronectin receptor or the phosphatidylserine receptor to recognize and remove apoptotic cells. *J. Immunol.* 149: 4029–4035.
16. Sanlioglu, S., C. M. Williams, L. Samavati, N. S. Butler, G. Wang, P. B. McCray, Jr., T. C. Ritchie, G. W. Hunninghake, E. Zandi, and J. F. Engelhardt. 2001. Lipopolysaccharide induces Rac1-dependent reactive oxygen species formation and coordinates tumor necrosis factor-α secretion through IKK regulation of NF-κB. *J. Biol. Chem.* 276: 30188–30198.
17. Leslie, C. C., and M. H. Gelb. 2004. Assaying phospholipase A2 activity. *Methods Mol. Biol.* 284: 229–242.
18. Varfolomeev, E. E., and A. Ashkenazi. 2004. Tumor necrosis factor: an apoptosis JuNKie? *Cell* 116: 491–497.
19. Schreck, R., P. Rieber, and P. A. Baeuerle. 1991. Reactive oxygen intermediates as apparently widely used messengers in the activation of the NF-κB transcription factor and HIV-1. *EMBO J.* 10: 2247–2258.
20. Goossens, V., K. De Vos, D. Vercammen, M. Steemans, K. Vancompernolle, W. Fiers, P. Vandenabeele, and J. Grooten. 1999. Redox regulation of TNF signaling. *Biofactors* 10: 145–156.
21. Piette, J., B. Piret, G. Bonizzi, S. Schoonbroodt, M. P. Merville, S. Legrand-Poels, and V. Bours. 1997. Multiple redox regulation in NF-κB transcription factor activation. *Biol. Chem.* 378: 1237–1245.
22. Baldwin, M. R., and J. T. Barbieri. 2005. The type III cytotoxins of *Yersinia* and *Pseudomonas aeruginosa* that modulate the actin cytoskeleton. *Curr. Top. Microbiol. Immunol.* 291: 147–166.
23. Williams, L. M., and A. J. Ridley. 2000. Lipopolysaccharide induces actin reorganization and tyrosine phosphorylation of Pyk2 and paxillin in monocytes and macrophages. *J. Immunol.* 164: 2028–2036.
24. Jupp, O. J., P. Vandenabeele, and D. J. MacEwan. 2003. Distinct regulation of cytosolic phospholipase A2 phosphorylation, translocation, proteolysis and activation by tumour necrosis factor-receptor subtypes. *Biochem. J.* 374: 453–461.
25. Jiang, Y. J., B. Lu, P. C. Choy, and G. M. Hatch. 2003. Regulation of cytosolic phospholipase A2, cyclooxygenase-1 and -2 expression by PMA, TNFα, LPS and M-CSF in human monocytes and macrophages. *Mol. Cell. Biochem.* 246: 31–38.
26. Nimnual, A. S., L. J. Taylor, and D. Bar-Sagi. 2003. Redox-dependent downregulation of Rho by Rac. *Nat. Cell Biol.* 5: 236–241.
27. Jin, L., Z. Ying, and R. C. Webb. 2004. Activation of Rho/Rho kinase signaling pathway by reactive oxygen species in rat aorta. *Am. J. Physiol.* 287: H1495–H1500.
28. Heo, J., and S. L. Campbell. 2005. Mechanism of redox-mediated guanine nucleotide exchange on redox-active Rho GTPases. *J. Biol. Chem.* 280: 31003–31010.
29. Rhee, S. G. 2006. Cell signaling: H_2O_2, a necessary evil for cell signaling. *Science* 312: 1882–1883.
30. Ridley, A. J., and A. Hall. 2004. Snails, Swiss, and serum: the solution for Rac 'n' Rho. *Cell* 116: S23–S25.
31. Etienne-Manneville, S., and A. Hall. 2002. Rho GTPases in cell biology. *Nature* 420: 629–635.
32. Wojciak-Stothard, B., A. Entwistle, R. Garg, and A. J. Ridley. 1998. Regulation of TNF-α-induced reorganization of the actin cytoskeleton and cell-cell junctions by Rho, Rac, and Cdc42 in human endothelial cells. *J. Cell. Physiol.* 176: 150–165.
33. Thannickal, V. J., and B. L. Fanburg. 2000. Reactive oxygen species in cell signaling. *Am. J. Physiol.* 279: L1005–L1028.
34. O'Donnell, V. B., S. Spycher, and A. Azzi. 1995. Involvement of oxidants and oxidant-generating enzyme(s) in tumour-necrosis-factor-α-mediated apoptosis: role for lipoxygenase pathway but not mitochondrial respiratory chain. *Biochem. J.* 310(Pt. 1): 133–141.
35. Chakraborti, S. 2003. Phospholipase A_2 isoforms: a perspective. *Cell. Signal.* 15: 637–665.
36. Theiss, A. L., J. G. Simmons, C. Jobin, and P. K. Lund. 2005. Tumor necrosis factor (TNF) α increases collagen accumulation and proliferation in intestinal myofibroblasts via TNF receptor 2. *J. Biol. Chem.* 280: 36099–36109.
37. Chan, F. K., J. Shisler, J. G. Bixby, M. Felices, L. Zheng, M. Appel, J. Orenstein, B. Moss, and M. J. Lenardo. 2003. A role for tumor necrosis factor receptor-2 and receptor-interacting protein in programmed necrosis and antiviral responses. *J. Biol. Chem.* 278: 51613–51621.
38. Schievella, A. R., J. H. Chen, J. R. Graham, and L. L. Lin. 1997. MADD, a novel death domain protein that interacts with the type 1 tumor necrosis factor receptor and activates mitogen-activated protein kinase. *J. Biol. Chem.* 272: 12069–12075.